3. GAS HOLDUP IN HIGH PRESSURE BUBBLE COLUMNS BY COMPUTED TOMOGRAPHY

3.1. Introduction

Two-phase bubble columns as well as three phase slurry bubble columns of various configurations have gained considerable attention in chemical industry due to their use in a number of processes, such as, Fischer-Tropsch synthesis, liquid phase methanol synthesis, wet oxidation of heavily polluted effluents, hydrogenation of heavy oils, etc. All of these processes operate at elevated pressure conditions (Deckwer, 1992). Most research on bubble columns has been performed at atmospheric conditions, and the scale-up and design of bubble columns at elevated pressures most often utilize the correlations that are based on data collected extensively at atmospheric conditions. This raises a question as to whether one can rely solely on the database established at atmospheric pressure. Jiang *et al.* (1995) observed that as pressure increases, the bubble size decreases, and the bubble size distribution becomes narrower. In an earlier study, Idogawa *et al.* (1986) observed that the behavior of bubbles depends closely on the type of gas distributor, and that this dependence weakened as the pressure increased. The effect vanished above 10 MPa. In the second study, Idogawa *et al.* (1987) reported that pressure had no effect on bubble diameter in bubble columns with gas superficial velocity in the range of 0.5 to 5.0 cm/s. In addition, Kölbel *et al*. (1961) found that gas holdup in a bubble column with a porous plate distributor was not affected by pressure in the range 0.1 MPa to 1.6 MPa when the superficial gas velocity, evaluated at the pressure in the column, was less than 3 cm/s. Deckwer *et al.* (1980) measured gas holdup in a slurry bubble column with a porous plate distributor containing fine particles at pressures up to 1.1 MPa and with superficial gas velocity below 4 cm/s. They also found no significant effect of pressure on gas holdup in that range of operating variables.

The main aim of this study is to investigate the effect of pressure on gas holdup over a broader range of superficial gas velocities using a non-intrusive technique, Computed Tomography (CT). Since the effect of column diameter on holdup profiles is still debated when using small diameter columns, holdup data was to be collected in a 6" diameter column which was constructed especially for this purpose at CREL-WU. A gamma ray based computer tomography system (CT) was developed (Kumar *et al*., 1995) for imaging phase holdup distribution in two-phase flow systems such as bubble columns and fluidized beds. The CT measurements were performed using an encapsulated γ-ray radiation source (Cs-137) and a fan beam arrangement of detectors. The details of the hardware and software have been described elsewhere (Kumar, 1994; Kumar *et al*., 1995, 1997) and will not be repeated here. Instead, the obtained experimental measurements for time averaged holdup cross-sectional distributions are discussed. The average cross-sectional holdup is compared to values obtained from various correlations.

3.2. **The High Pressure Experimental Facility**

Figure 3.1 displays the flowsheet for the high pressure system used in this study. The system is designed to handle a high flow rate of air up to 5000 SCFH at a pressure of up to 175 psig. All the equipment is designed to support 200 psig. The bubble column is made of a stainless steel tube with inner diameter 0.169 m (6.359”), and height 2.5 m (8.2 ft). Figure 3.2 shows the sketch of the column including the bottom flange which has been modified to serve as a support as well. Figure 3.3 shows the sketch of the elevation of the column along the section AA as indicated on the schematic of Figure 3.2.

As shown in Figure 3.3, a transparent glass window is situated at the top of the column and is named “blue eye”. This window allows viewing the system before starting the CT scan. The gas was dispersed into the column through a perforated plate distributor. The distributor, shown schematically in Figure 3.4, has 61 holes each of 0.4 mm diameter, providing an open area of 0.05%. The holes are arranged in 3 concentric circles with 20 holes on each circle and one at the center of the distributor plate. The increment in radius between the circles on which holes are centered is 1.5 cm. This particular distributor was used because a significant amount of data for holdup distribution and liquid velocity is available for it from our previous studies. Table 3.1 lists the operating conditions used in this study.

Air was used as the gas phase. As the liquid phase, tap water (σL = 72 mN/m, μL = 993 μPa.s) was used. The experiments were conducted batchwise with respect to the liquid, but with a continuous flow of gas at ambient temperature (T = 25 °C). Air was filtered before being introduced into the system. The gas flow rate was controlled by the rotameters at the desired values. After exiting the bubble column, the gas passes through a back-pressure regulator, which is used to control the pressure in the column. It is then discharged into the atmosphere through the vent. Two pressure safety valves are mounted both at the top and bottom of the column to prevent accidental over-pressurization.

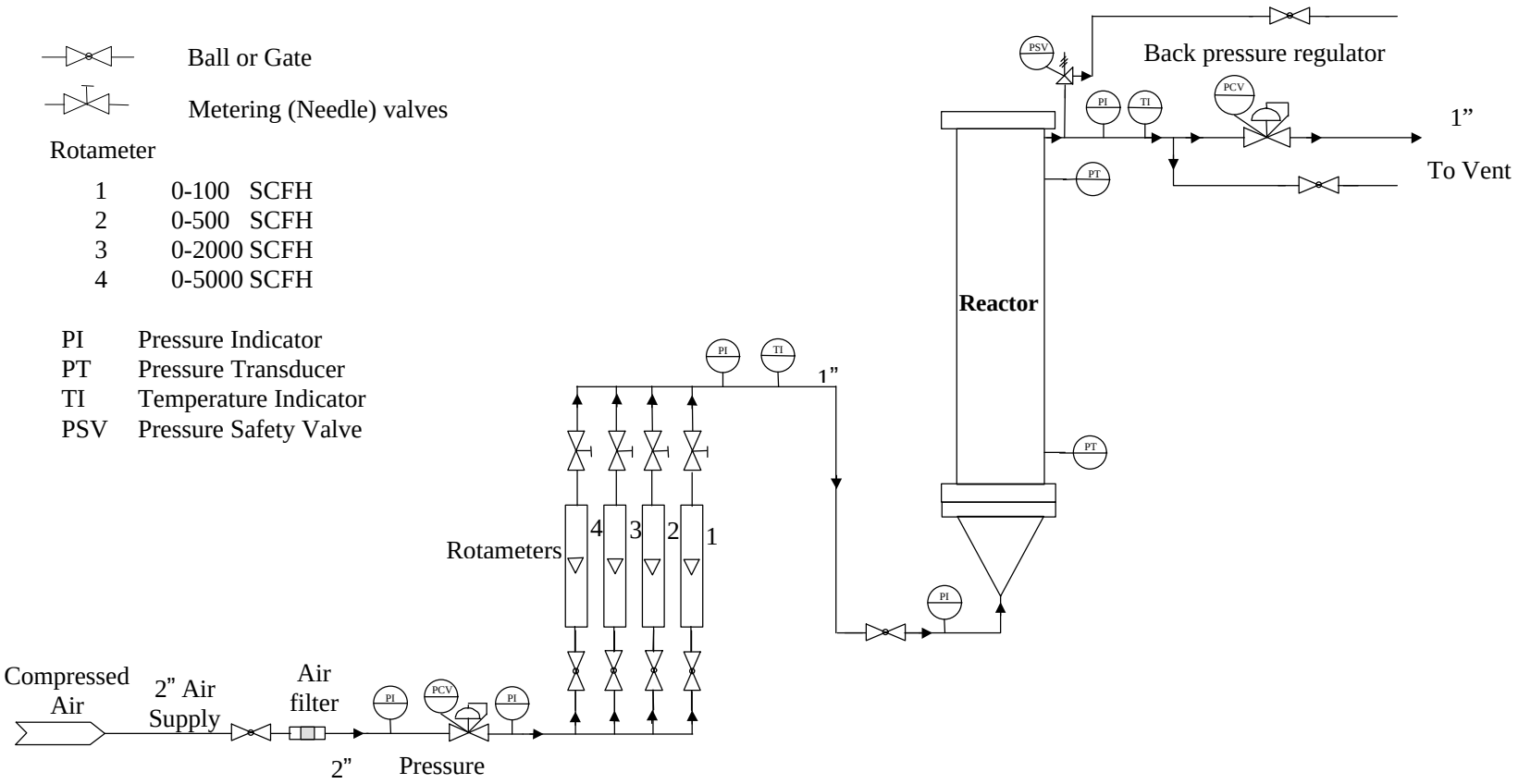

Figure 3.1 : Flowsheet for High Pressure Column

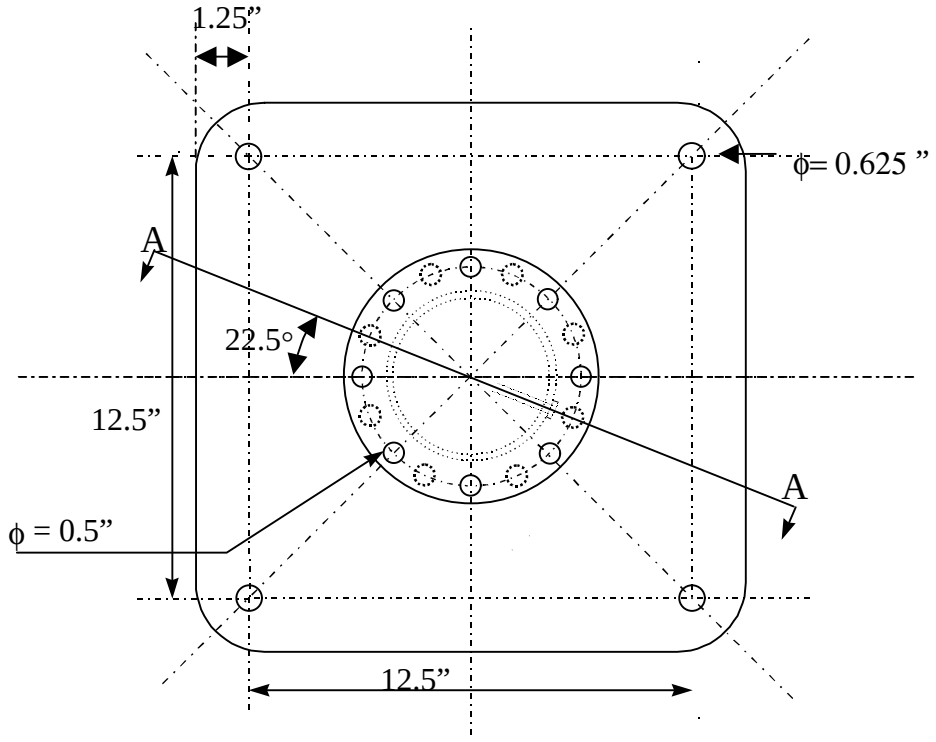

Figure 3.2: Top View of the High Pressure Column

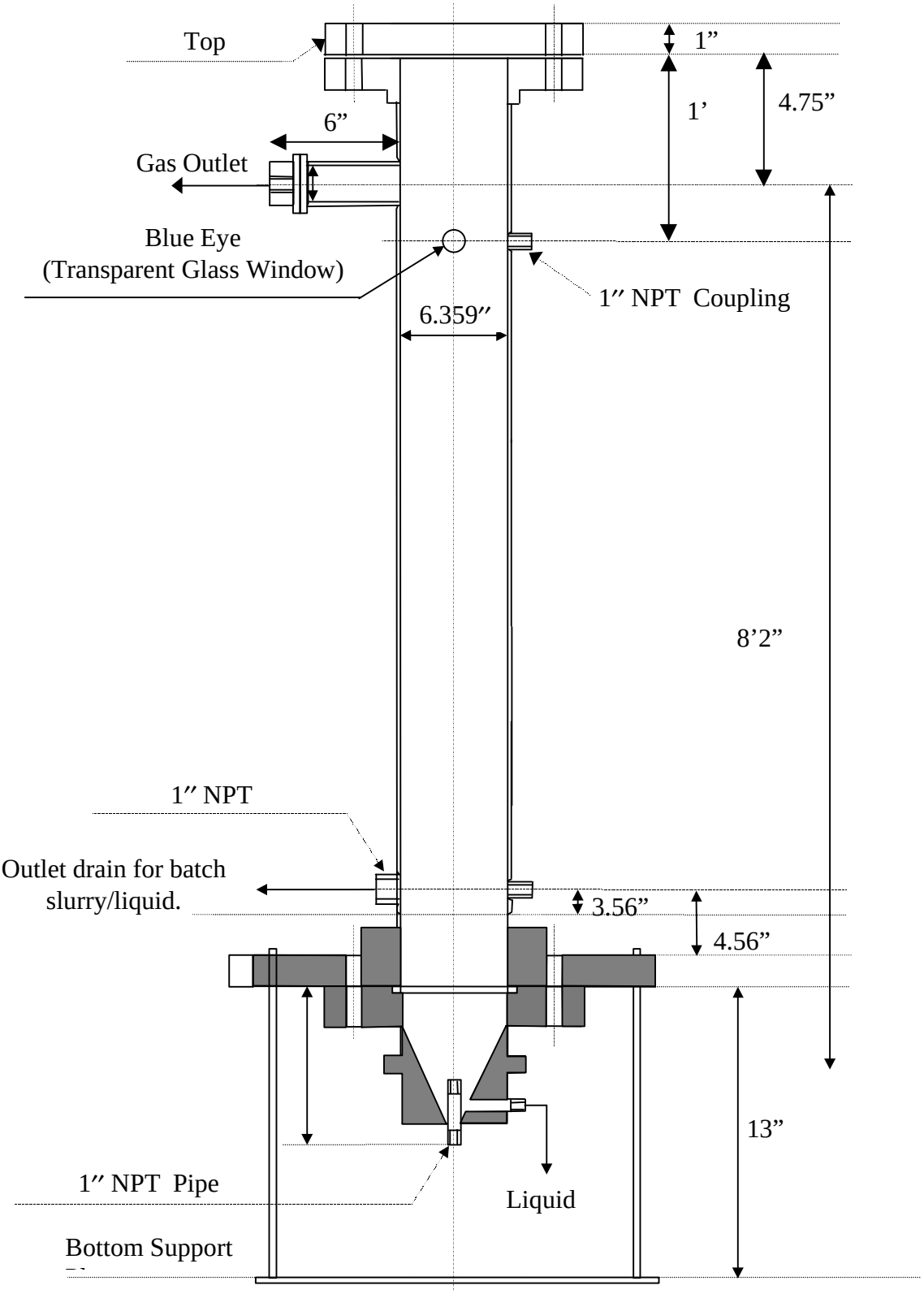

Figure 3.3: Side View of the High Pressure Bubble Column Elevation Along Section AA of Figure 3.2

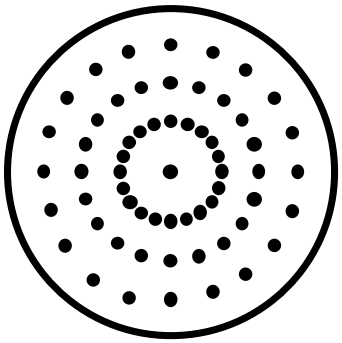

Figure 3.4: Perforated Plate Distributor of 0.04% Open Area

Table 3.1: Operating Conditions for the High Pressure System

Diameter of column, in. (cm)	6.359 (16.15)
Distributor	Perforated plate with 61 holes (each of 0.4 mm diameter), open area 0.05% (Fig. 3.4)
Superficial gas velocity, cm/s	2, 5, 12, 18
Liquid (water)	Batch
Pressure, MPa (atm)	0.1 (1), 0.3 (3), 0.7 (7)
Temperature, ° C	25

As already mentioned in this study the gas holdup cross-sectional distribution was measured using the gamma ray scanner and the associated tomography reconstruction algorithms developed in CREL and discussed by Kumar *et al.* (1995; 1997). The CREL scanner is a versatile instrument that enables the quantification of the time-averaged holdup distribution for two-phase flows under a wide range of operating conditions. The fan beam configuration of the scanner consists of an array of NaI detectors of 5 cm in diameter (5 detectors were used in this study), and an encapsulated 100 mCi Cs^{137} source located opposite to the center of the array of detectors. The measurements can be performed at different axial elevations. In this study, gas holdup distribution was measured at about 3 feet from the distributor where the flow is fully developed..

3.3. Results and Discussion

3.3.1. Radial Gas Holdup Distribution

Figures 3.5 and 3.6 display the radial gas holdup distribution at different operating pressures each at a different superficial gas velocity. These plots were obtained by azimuthally averaging the CT measured holdup distribution in the cross-section of the column 3 feet above the distributor. Our past experience indicates that at L/D ratio of 6 or above, the holdup profile is well-developed and relatively invariant to axial position

(Kumar, 1994). From these figures, it can be seen that the differences in holdup profiles due to pressure increase with increasing superficial gas velocity.

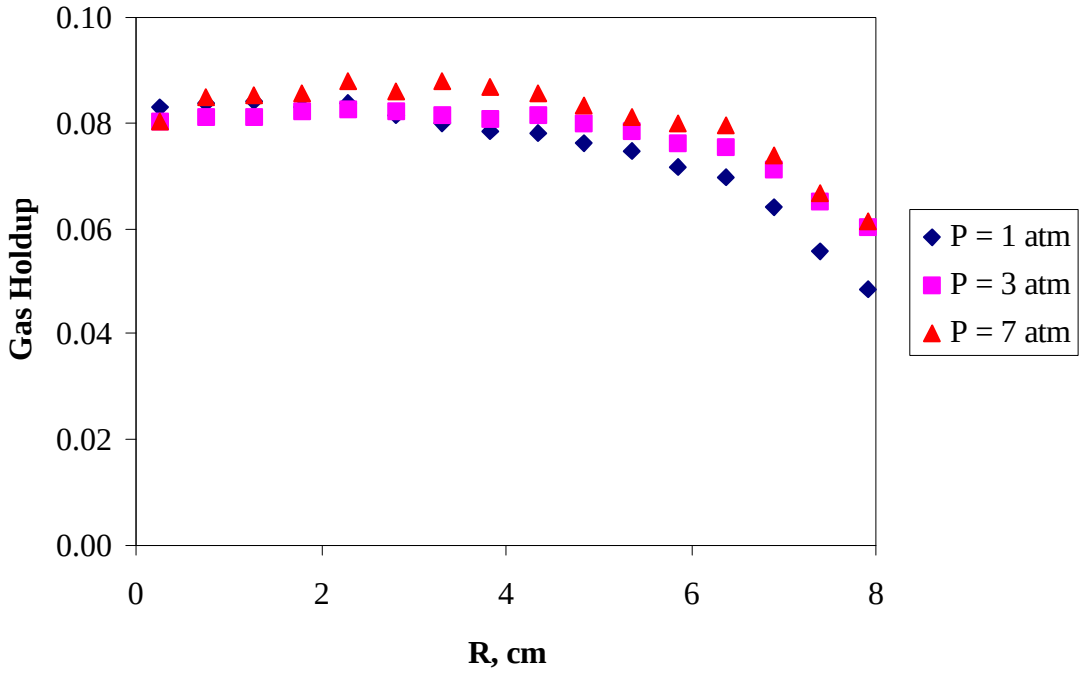

Figure 3.5: Radial Gas Holdup Distribution as a Function of Pressure for U_g = 2 cm/s

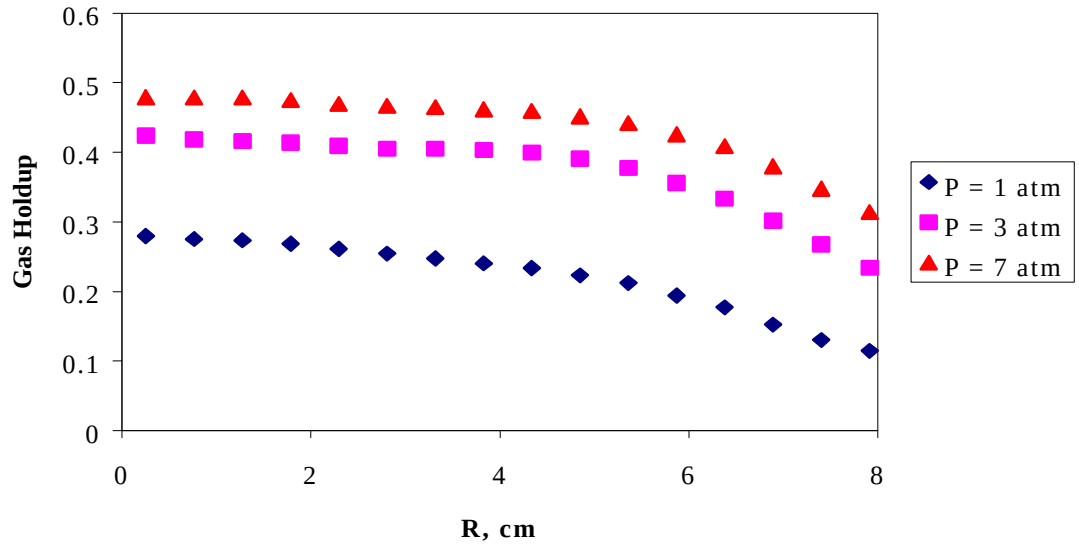

Figure 3.6: Radial Gas Holdup Distribution as a Function of Pressure for U_g = 12 cm/s

Figure 3.7 displays the results obtained by Shollenberger *et al*. (1995) at atmospheric conditions. The trend in gas holdup at atmospheric pressure with increasing superficial gas velocities observed by us agrees well with their results. However, the gas holdup obtained in this study is slightly higher than that from Shollenberger *et al*. For example, at a superficial gas velocity of 11.76 cm/s, the gas holdup value at the center, reported by Shollenberger et al., is about 0.205 (Figure 3.7), whereas in our case, a center line gas holdup value of about 0.28 is obtained at superficial gas velocity of 12 cm/s (Figure 3.6). The discrepancies might be due to the type of distributor used or quality of water. Shollenberger *et al*. used a bubble cap distributor, whereas in this study a perforated plate with more holes in the center, which might enhance a non-uniform distribution, was used.

From Figures 3.5 and 3.6, it is evident that gas holdup increases both with pressure, and with superficial gas velocity in agreement with the reports in the literature (Idogawa *et al*., 1986, Jiang *et al*., 1995, Kojima *et al.*, 1991, Kojima *et al*., 1987, Lin *et al*. (1998), and Oyevaar *et al*., 1989). At a velocity of 12 cm/s (Figure 3.6), the radial gas holdup profile at atmospheric pressure is distinctly parabolic in nature, indicating churn turbulent flow, whereas at higher pressure, the profile is flatter. However, Shollenberger *et al.* (1996; 1997), who used a different gamma tomography system, report somewhat different observations. This can be seen in Figure 3.8, which displays the radial gas holdup distribution at 10 cm/s superficial gas velocity in of a 0.48 m ID and 3 m tall column, where they found that the gas holdup profile is parabolic at a pressure of 0.394 MPa. In their study, the sparger was a 15 cm diameter ring formed from 1.1-cm ID stainless steel tubing. There were 12 holes equidistantly distributed on the ring, each of 3.18 mm in diameter. Hence, the discrepancies might be due also to the type of distributor and size of column used. The exact cause is not known at present.

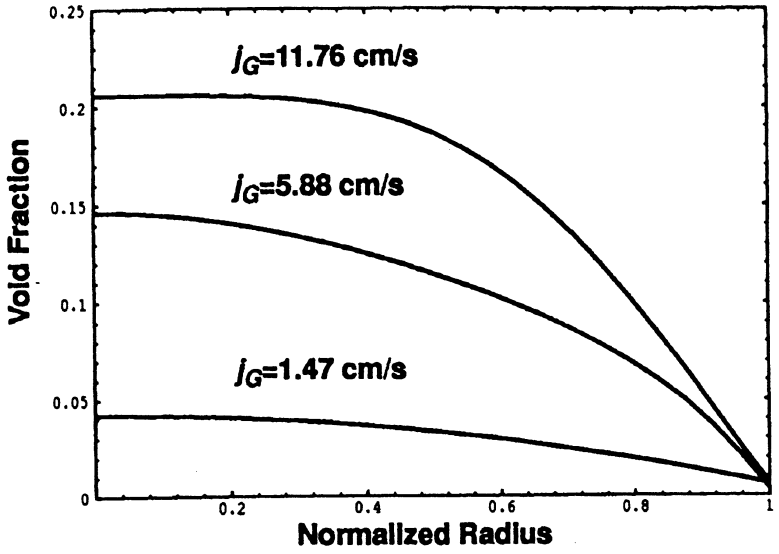

Figure 3.7: Radial Distribution of Gas Holdup at Atmospheric Conditions as a Function of Superficial Gas Velocity for 19 cm Air-Water Column with Bubble Cap Distributor (Shollenberger *et al*., 1995)

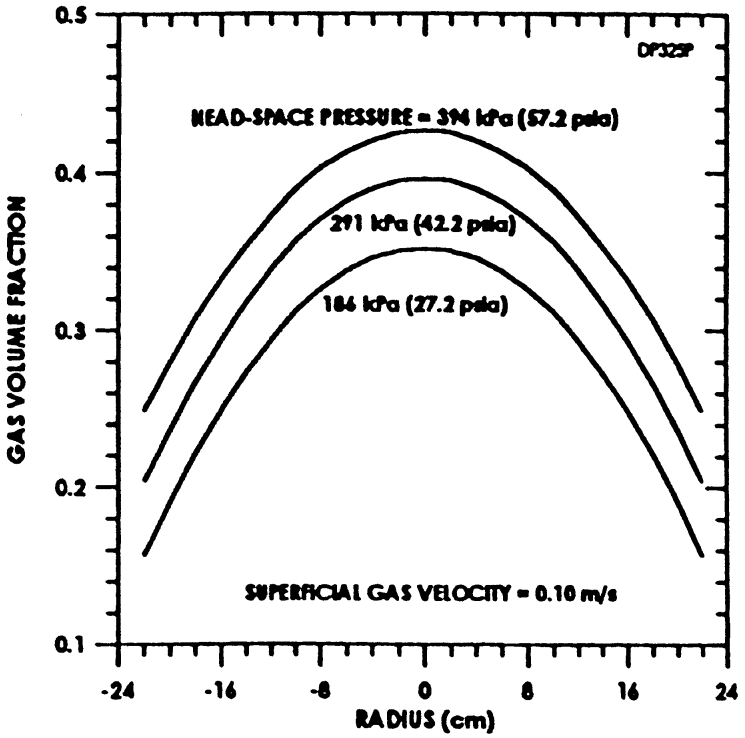

Figure 3.8: Radial Distribution of Gas Holdup as a Function of Pressure for Ug = 10 cm/s (Taken from Shollenberger *et al*., 1996)

Figures 3.9 and 3.10 display the cross-sectional distribution of the gas holdup for the bubble column at different pressures for two superficial gas velocity studied. For example, Figure 3.9 (a) shows the pixel map for P = 1 atm, and U_g = 2 cm/s. The map indicates that gas holdup at these conditions has a maximum value of 0.1, and this occurs near the center of the column, which shows a darker area. With this interpretation, one can see that as the gas superficial velocity and column pressure increase, gas holdup increases (Figure 3.10 (d)).

Thus, a gradual variation in the color shades for the gas holdup from the column center to the wall indicates a change in gas holdup value. These plots confirm that gas holdup increases with pressure and superficial gas velocities. Visual observations of the column in the vicinity of the wall via the "blue eye" revealed much smaller bubbles when pressure is increased. The coalescence rate seems to be decreased and bubble breakup seems promoted at pressurized conditions. Hence, gas holdup increases as pressure increases.

3.3.2. Cross-Sectional Average Gas Holdup

The cross-sectional averaged gas holdup is calculated using Equation (3.1) and can be taken as a good estimate of the overall gas holdup (Kumar, 1994).

$$\bar{\varepsilon}_g = \frac{2}{R^2}\int_0^R r\varepsilon(r)dr \qquad (3.1)$$

Figure 3.11 displays the cross-sectional average gas holdup as a function of superficial gas velocity at various pressures, while Figure 3.12 displays the given data for the cross-sectional average gas holdup as a function of pressure at different superficial gas velocities. Table 3.2 lists the calculated cross-sectional average gas holdup values for different operating conditions.

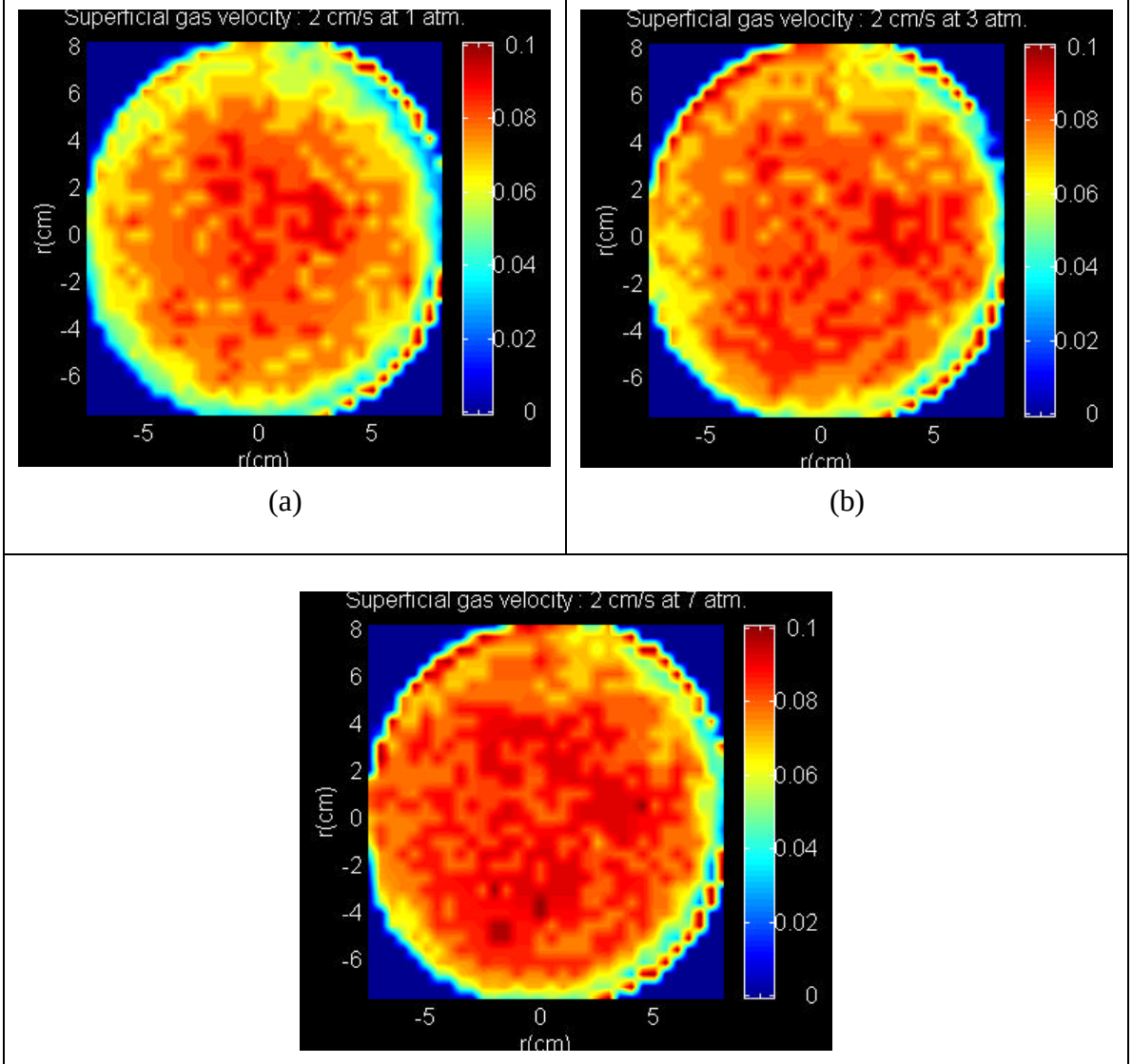

(a) (b)

(c)

Figure 3.9: Cross-sectional Distribution of the Gas Holdup at (a) P = 1 atm, (b) P = 3 atm, and (c) P = 7 atm for U_g = 2 cm/s

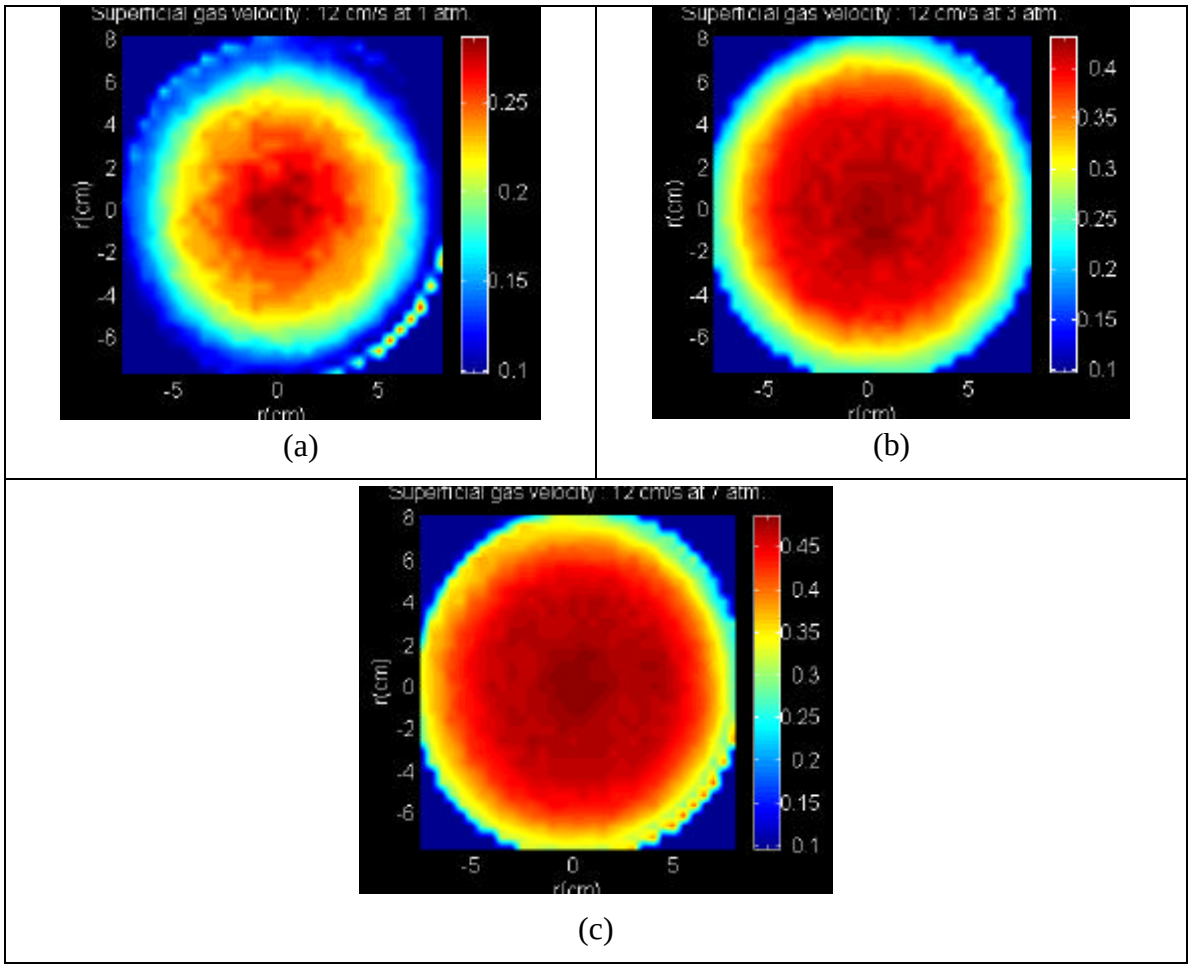

Figure 3.10: Cross-sectional Distribution of the Gas Holdup at (a) P = 1 atm, (b) P= 3 atm, and (c) P = 7 atm for U_g = 12 cm/s

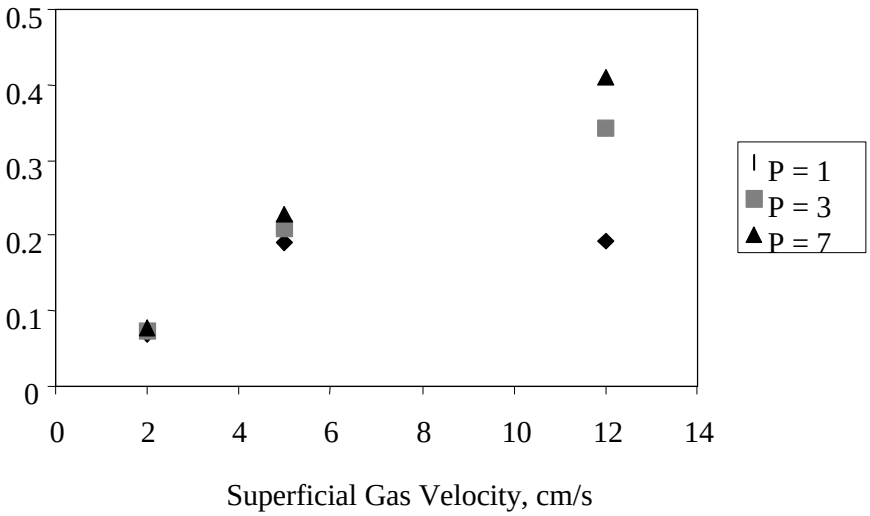

Figure 3.11: Cross-sectional Average Gas Holdup as a Function of Superficial Gas Velocity at Different Pressures

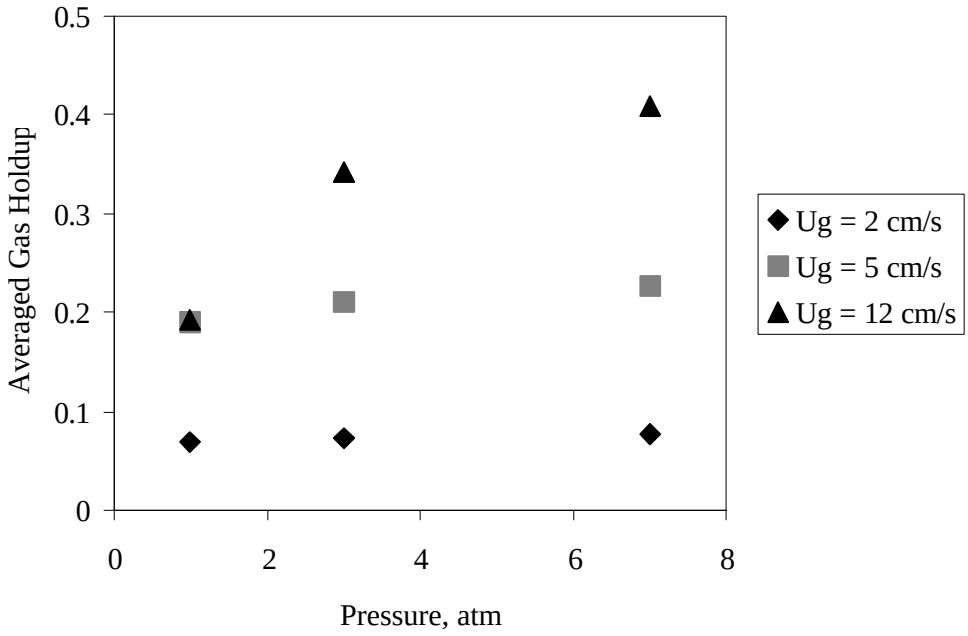

Figure 3.12: Cross-sectional Averaged Gas Holdup as a Function of Pressure at Different Superficial Gas Velocities

Table 3.2: Cross-Sectional Average Gas Holdup at Different Operating Conditions

Pressure, atm	Superficial gas velocity, cm/s	$\bar{\varepsilon}_g$
1	2	0.069
	5	0.191
	12	0.193
3	2	0.074
	5	0.210
	12	0.342
7	2	0.077
	5	0.227
	12	0.410